Journal of Fluency Disorders 55 (2018) 68–83

Contents lists available at ScienceDirect

Journal of Fluency Disorders

journal homepage: www.elsevier.com/locate/jfludis

White matter pathways in persistent developmental stuttering: Lessons from tractography

Vered Kronfeld-Duenias[a,*], Oren Civier[a,1], Ofer Amir[b], Ruth Ezrati-Vinacour[b], Michal Ben-Shachar[a,c,*]

[a] The Gonda Multidisciplinary Brain Research Center, Bar-Ilan University, Ramat-Gan, Israel
[b] The Department of Communication Disorders, Sackler Faculty of Medicine, Tel-Aviv University, Israel
[c] The Department of English Literature and Linguistics, Bar-Ilan University, Ramat-Gan, Israel

ARTICLE INFO

Keywords:
fluency disorders
stuttering
diffusion imaging
tractography
white matter
methodological overview

ABSTRACT

Purpose: Fluent speech production relies on the coordinated processing of multiple brain regions. This highlights the role of neural pathways that connect distinct brain regions in producing fluent speech. Here, we aim to investigate the role of the white matter pathways in persistent developmental stuttering (PDS), where speech fluency is disrupted.

Methods: We use diffusion weighted imaging and tractography to compare the white matter properties between adults who do and do not stutter. We compare the diffusion properties along 18 major cerebral white matter pathways. We complement the analysis with an overview of the methodology and a roadmap of the pathways implicated in PDS according to the existing literature.

Results: We report differences in the microstructural properties of the anterior callosum, the right inferior longitudinal fasciculus and the right cingulum in people who stutter compared with fluent controls.

Conclusions: Persistent developmental stuttering is consistently associated with differences in bilateral distributed networks. We review evidence showing that PDS involves differences in bilateral dorsal fronto-temporal and fronto-parietal pathways, in callosal pathways, in several motor pathways and in basal ganglia connections. This entails an important role for long range white matter pathways in this disorder. Using a wide-lens analysis, we demonstrate differences in additional, right hemispheric pathways, which go beyond the replicable findings in the literature. This suggests that the affected circuits may extend beyond the known language and motor pathways.

Persistent developmental stuttering (PDS) is a speech impairment that disrupts fluent speech production in around 1% of the adult population (Yairi & Ambrose, 1999). Over the years, many attempts have been made to target the neurological underpinnings of PDS using structural and functional imaging methodologies. Here, we report novel findings from a tractography analysis of 18 major white matter pathways segmented in a sample of adults who do and do not stutter. We complement the analysis with an overview of the methodology and existing literature on white matter tracts affected in PDS. We discuss our findings within the context of this literature, and assess the strengths and weaknesses of tractography as a research tool for understanding the white matter properties of people who stutter.

* Corresponding authors at: The Gonda Multidisciplinary Brain Research Center, Bar-Ilan University, Ramat-Gan 5290002, Israel.
E-mail addresses: vered.kronfeld@gmail.com (V. Kronfeld-Duenias), michalb@mail.biu.ac.il (M. Ben-Shachar).
[1] Current affiliation: The Florey Institute of Neuroscience and Mental Health, Melbourne Brain Centre, Melbourne, Australia.

http://dx.doi.org/10.1016/j.jfludis.2017.09.002
Received 1 September 2016; Received in revised form 18 April 2017; Accepted 5 September 2017
Available online 13 September 2017
0094-730X/

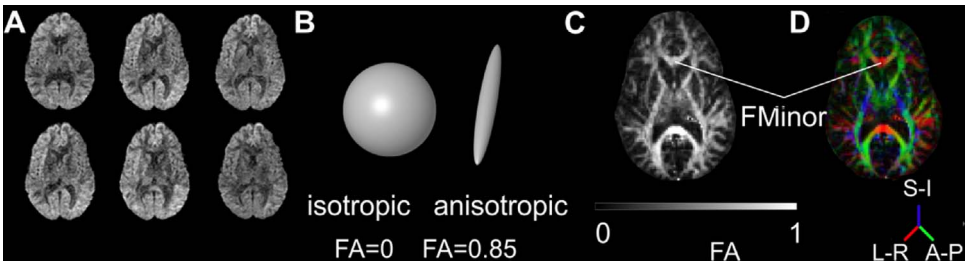

Fig. 1. Main concepts of DTI. (A) Six raw images of the same axial slice (roughly Z = 5 in standard MNI space) are shown in a representative participant. Each image captures the degree of diffusion in a single direction. A non-weighted volume (B0) is also collected as reference. (B) In each voxel, the diffusion measurements along the different directions are modeled as a tensor. Isotropic diffusion is modeled as a perfect sphere (left) and anisotropic diffusion is modeled as an elongated ellipsoid (right). (C) FA map in a single slice. The FA values probe the directionality of the underlying tissue, ranging between 0 and 1. The higher the FA, the brighter the image. For illustration, the anterior callosum (FMinor), that is highly anisotropic, is labelled. (D) The principal diffusion direction of each voxel in the same axial slice as in (C) is color-coded based on the following scheme: superior-inferior (blue), left-right (red), anterior-posterior (green). The mid sagittal segment of the anterior callosum (labelled) appears in red, in accordance with the left- right orientation. *Abbreviations*: fractional anisotropy (FA), anterior (A), posterior (P), left (L), right (R), superior (S), inferior (I). For interpretation of the references to color in this figure legend, the reader is referred to the web version of this article.

Why white matter?

Over the last 20 years, functional imaging studies have reported atypical activation patterns that accompany speech production in people who stutter in a wide range of brain regions, including the left primary motor and premotor cortices, right primary motor cortex and inferior frontal gyrus, supplementary and pre-supplementary motor areas, bilateral auditory cortices, the cerebellar vermis and several basal-ganglia structures (see meta-analyses by Belyk, Kraft, & Brown, 2015; Brown, Ingham, Ingham, Laird, & Fox, 2005; Budde, Barron, & Fox, 2015). This wide-spread pattern of affected regions is expected, because speech production relies on the coordinated processing of multiple, often distant, brain regions (Golfinopoulos, Tourville, & Guenther, 2010). Notably, however, this distributed map suggests an important role for neuronal (mis)communication in PDS.

White matter constitutes one of the major tissue types in the brain. It is composed of bundles of nerve cell projections (axons) that connect nerve cell bodies to one another. A bundle of nerve cell projections that connects distinct populations of nerve cell bodies is typically called a ‘pathway’ or a ‘fiber tract’. The anatomical literature distinguishes between pathways that connect neighboring nerve cell bodies (‘short-range fibers’ or ‘U-fibers’), pathways that connect distant nerve cell bodies within a hemisphere (‘long-range fibers’) or those connecting between the two hemispheres (‘commissural fibers’). Together, the white matter pathways constitute the infrastructure that supports neuronal communication, hence their functioning is of great importance in clinical conditions where multiple brain regions are involved, such as PDS.

Measuring white matter properties non-invasively in healthy humans

Diffusion Magnetic Resonance Imaging (dMRI) is currently the most common methodology for the study of white matter in brain research in living humans. Briefly, this methodology measures the speed of free diffusion of water molecules in brain tissue, as a tool to probe the microstructural properties of their surrounding medium. The average speed of water diffusion differs between brain tissues: faster (around 2.5 μm/s) in regions filled with cerebro-spinal fluid (CSF), where there are less barriers to diffusion, and slower (1.7 μm/s) in white matter, where cell membranes and fatty myelin wraps constrain diffusion (Le Bihan et al., 1986).

Of great importance for our purposes are differences in the anisotropy (directionality) of water diffusion between and within different brain tissues. Water diffusion within the large bundles of axons that make up the white matter is typically faster parallel to the axons and slower perpendicular to them, resulting in an anisotropic pattern of diffusion (Basser, 1995; Basser, Mattiello, & LeBihan, 1994; Basser & Pierpaoli, 1996). In contrast, water diffusion in the gray matter or in CSF proceeds at roughly equal speed in different directions, resulting in an isotropic diffusion pattern. By measuring the average speed of diffusion, its anisotropy and directional distribution, we may thus probe the microstructural properties of white matter tissue.

In dMRI, we collect images sensitized to the speed of water diffusion along a specific direction, and repeat these measurements along multiple directions (see Fig. 1A). The raw data is first preprocessed to correct for head-motion and other image distortions.[2] Then, a mathematical model is used to describe the pattern of diffusion in each voxel[3] of these images. The simplest and still most popular model of diffusion is the tensor model (Basser et al., 1994). The tensor model can be visually represented as an ellipsoid pointing in the direction of fastest diffusion (termed ‘the principal diffusion direction’). An elongated cigar-shaped ellipsoid represents highly anisotropic diffusion, while a perfect sphere represents isotropic diffusion (illustrin Fig. 1B). Formally, a tensor can be fully characterized by three orthogonal vectors (eigenvectors), each identified by its direction and by its magnitude, which represents the diffusion speed along that direction. The term ‘Diffusion Tensor Imaging’ (DTI) refers to dMRI data modeled, at the voxel level, by tensors.

[2] Corrections for head motion and eddy-current distortions are performed by registering each image to the first or mean image. These processes involve interpolation and thus may introduce some smoothing beyond the original resolution of the raw data.

[3] Brain images represent slices of some thickness. Therefore, their pixels are called ‘voxels’, for volume-picture-elements.

Several parameters are typically obtained from the tensors in order to quantify the microstructural properties of the underlying tissue. Of these, fractional anisotropy (FA) is the most popular summary measure. FA is defined as the normalized standard deviation of the magnitudes of the tensor's three eigenvectors (Basser et al., 1994). It describes how different the diffusion speed is along the orthogonal directions that define the tensor, therefore providing a measure of the degree of directionality, or anisotropy, of the underlying tissue. FA values range from 0 to 1, where 0 indicates a perfect sphere (isotropic diffusion) and 1 indicates an infinitely elongated, cigar-shaped ellipsoid (anisotropic diffusion, see Fig. 1C). Other commonly used parameters include axial diffusivity (AD) that refers to the magnitude of the largest diffusion vector, radial diffusivity (RD) that refers to the average magnitude of the secondary two vectors, and mean diffusivity (MD) that refers to the average magnitude of all three vectors.

Maps charting the distribution of FA, MD, AD and RD across the white matter can be used to detect regions that show significant differences between clinical samples and their matched controls. Alternatively, these maps can be used to identify regions that demonstrate associations between the microstructural properties of the brain tissue in a specific brain location and behavioral measures (e.g., individual fluency scores) assessed outside the scanner in the same individuals. Different measures of diffusivity (e.g., FA vs. MD) provide complementary information about the shape of the tensor and presumably about the microstructural properties of the underlying tissue. FA quantifies how elongated the tensor is, and is commonly referred to as a summary measure of the overall directionality of the tissue. MD measures how large the tensor is, and provides an estimation of the overall tissue density (Pierpaoli & Basser, 1996). AD and RD complement this picture by providing a more direct measure of the diffusion in the main direction of the white matter pathway and perpendicular to it, respectively. Simultaneous use of multiple metrics allows better characterization of the underling tissue (Alexander et al., 2012; Alexander, Lee, Lazar, & Field, 2007) and the choice of one metric over another also depends on the research question and sample characteristics. MD, for example, is most sensitive to group effects in small samples (De Santis, Drakesmith, Bells, Assaf, & Jones, 2014).

The tensor model has revolutionized the field of white matter research by providing researchers with a simple and elegant model of water diffusivity that can be captured in diffusion data measured along as little as 6 non-collinear directions. Still, the tensor model suffers from several limitations, particularly in regions of crossing fibers. In such regions, single voxels may contain more than one principal fiber orientation, but this complexity is not well modeled by a single ellipsoid.

To address this issue (and others that exceed the scope of this paper) alternative modeling approaches have been introduced. Some of these models use explicit assumptions about the signal, for example, the Composite Hindered and Restricted Model of Diffusion approach produces separate estimates for intra- and extra- axonal tissue compartments (CHARMED; Assaf & Basser, 2005), and the "ball and stick" model assumes anisotroic diffusion within the axons (stick) and isotropic diffusion outside axons (ball) (Behrens et al., 2003). Other models allow for more than one dominant fiber orientation, for example, multi-tensor models (Behrens, Berg, Jbabdi, Rushworth, & Woolrich, 2007), Q-ball imaging (Tuch, 2004), diffusion spectrum imaging (DSI; Wedeen, Hagmann, Tseng, Reese, & Weisskoff, 2005), and constrained spherical deconvolution (CSD; Tournier et al., 2008). These models have the potential to resolve some of the limitations of the tensor model and therefore they are becoming more popular. Their advantages come at a cost of scan time and computational resources, but their popularity is expected to grow with improvements in MRI technology and in computing power (see Rokem et al., 2015; Tournier, Mori, & Leemans, 2011 for more discussion on this topic).

White matter regions implicated in voxel-based comparisons in PDS

Several studies have used voxel-based comparisons of diffusion data between groups of adults who do and do not stutter, to evaluate PDS-related white matter differences. In voxel-based analyses, the diffusion data of each participant is registered to a standard space via mutual information maximization (e.g., using SPM's Voxel Based Analysis toolbox by Penny, Friston, Ashburner, Kiebel, & Nichols, 2011) or through methods specifically designed for white matter registration (e.g., Tract Based Spatial Statistics (TBSS) by Smith et al., 2006; see more on TBSS in). Then, summary measures such as FA or MD are compared between the groups in template space, in a voxel-by-voxel fashion. High quality registration and proper correction for multiple comparisons (across tens of thousands of voxels) are therefore key to such analyses.

The earliest and most well established voxel-based finding in the study of white matter properties in PDS indicates that individuals who stutter have lower FA values compared with controls in the white matter underneath the left Rolandic operculum (RO), a left frontal region below the sensorimotor representation of the oropharynx at the level of the central sulcus (Sommer, Koch, Paulus, Weiller, & Büchel, 2002). Over the years, this finding was replicated multiple times in adults and children who stutter (Chang, Erickson, Ambrose, Hasegawa-Johnson, & Ludlow, 2008; Connally et al., 2014; Cykowski, Fox, Ingham, Ingham, & Robin, 2010; Watkins, Smith, Davis, & Howell, 2008). While there is great variability in the precise location of the group difference across different reports (see, for example, Fig. 2 of Cykowski et al., 2010), FA reduction in left frontal regions around the left RO is considered the most replicable finding in this literature.

Another replicable voxel-based difference between people who stutter and controls is seen in FA values in the corpus callosum. As in the case of the left RO, there is little consistency with regards to the exact location of this finding: while some studies indicate a difference in the anterior callosum (Cai et al., 2014; Civier, Kronfeld-Duenias, Amir, Ezrati-Vinacour, & Ben-Shachar, 2015; Cykowski et al., 2010; Kell et al., 2009), others report a difference in the posterior callosum (Chang, Zhu, Choo, & Angstadt, 2015; Connally et al., 2014; Neef, Anwander, & Friederici, 2015). Most of these studies agree on the direction of the effect, reporting FA *reduction* in the callosum of individuals who stutter compared with controls (but see Kell et al., 2009).

Atypical white matter properties are further reported in multiple widespread brain regions. A partial list of these regions includes bilateral white matter regions underneath the precentral gyrus (Chang et al., 2015; Connally et al., 2014; Watkins et al., 2008), white matter within bilateral cerebellar peduncles (Connally et al., 2014; Watkins et al., 2008), white matter underneath the left

supramarginal gyrus (Chang et al., 2015; Watkins et al., 2008) and regions within the bilateral corticospinal tracts (CST) (Cai et al., 2014; Chang et al., 2008; Connally et al., 2014; Watkins et al., 2008). The diffuse and variable nature of the findings was recently illustrated in a meta-analysis (see Fig. 1 of Neef et al., 2015). It is further discussed by Etchell et al., in this special issue (this volume).

From voxels to virtual trajectories: motivation and main concepts of tractography

The studies described so far have established PDS-related differences in the microstructural properties of white matter, in support of the broad hypothesis that PDS involves altered connectivity between distant brain regions. However, mapping voxel-based differences to implicated pathways is complicated. This is because voxel-based methods detect differences in specific coordinates in standard (template) space, but these coordinates may map to different tracts in different individuals, due to individual differences in brain anatomy, shape and size. Moreover, mapping an affected cluster to a specific pathway is, in many cases, complicated.

Consider, for example, the common finding of FA reduction underneath the left RO in PDS (Chang et al., 2008; Connally et al., 2014; Cykowski et al., 2010; Sommer et al., 2002; Watkins et al., 2008). Typically, differences in the left RO were interpreted as differences in the superior longitudinal fasciculus/arcuate fasciculus (Chang et al., 2008; Connally et al., 2014; Cykowski et al., 2010; Watkins et al., 2008). However, given that the frontal lobe is packed with long- and short- range connections (Catani et al., 2012; Thiebaut de Schotten, Dell'Acqua, Valabregue, & Catani, 2012), FA reductions in this region may also be associated with differences in shorter connections between the sensorimotor cortex and the frontal operculum or ventral premotor cortex (see Fig. 1 of Kronfeld-Duenias, Amir, Ezrati-Vinacour, Civier, & Ben-Shachar, 2016a).

To date, the most common methodology for identifying specific pathways in living humans is tractography. Tractography is a computational process in which the diffusion data is used to reconstruct continuous 3D trajectories (virtual fibers) based on local estimates of fiber orientations. Tract reconstruction is performed in the native space of each participant, which makes this methodology less susceptible to inter-subject registration errors, providing increased sensitivity relative to voxel-based methods: (see Ben-Shachar, Dougherty, & Wandell, 2007 for a detailed discussion).

Tractography algorithms can be divided broadly into two categories: deterministic and probabilistic. In deterministic tractography, a pathway is propagated from a seed point positioned within a voxel, along the principal diffusion direction of the tensor in that voxel. This process proceeds to connect multiple points in space into a virtual fiber, until some termination criterion (determined a-priori by the experimenter) is reached. For example, when the FA of the next tensor is too low to rely on the direction in which it points with confidence, or when the angle between the current direction and the direction of the next tensor is too sharp. The distinction between deterministic and probabilistic algorithms emerges in voxels that contain distinct subpopulations of axons along different directions. When a deterministic algorithm reaches such a voxel, it follows only one of these directions (the principal direction of the tensor). However, a probabilistic algorithm proceeds along multiple pathway propagation directions, generating multiple fibers, based on the measured distribution of fiber orientations (Behrens et al., 2007; Sherbondy, Dougherty, Ben-Shachar, Napel, & Wandell, 2008; Tournier, Calamante, Gadian, & Connelly, 2004).

Deterministic tractography produces reliable tract estimates in many regions within the core white matter of the brain (Danielian, Iwata, Thomasson, & Floeter, 2010; Dougherty, Ben-Shachar, Bammer, Brewer, & Wandell, 2005), but fails to produce an accurate depiction of white matter pathways in regions of crossing and kissing fibers (Buchanan, Pernet, Gorgolewski, Storkey, & Bastin, 2014). Probabilistic tractography addresses some of the limitations of deterministic tractography by providing information about the likelihood of connections between seed and target voxels. However, probabilistic tractography is computationally more complex and prone to difficulties in identifying fiber terminations, which may result in reproducible but erroneous trajectories (see, for example, Fig. 10 of Jones, 2008; Pestilli, Yeatman, Rokem, Kay, & Wandell, 2014).

The choice of a tractography algorithm is related to, but distinct from, the choice of the diffusion model at the voxel level. While the diffusion model provides a compact description of the diffusion pattern at each point in space, the tractography algorithm determines the propagation procedure from one point to another. Simple diffusion models like the tensor do not provide rich enough information for probabilistic algorithms to pursue multiple pathway propagation options. More complex diffusion models, such as CSD, combine more naturally with probabilistic tractography algorithms, but require measurements along 45 directions or more, resulting in much longer scan time (see Jones, 2008 for a comprehensive review of tractography).

Following tract identification using tractography, the diffusion properties (FA, MD, AD, RD) can be extracted from the voxels traversed by the tract's virtual pathway, either as an average across all voxels traversed by the tract or as a profile of values assessed at multiple points along the tract, for each individual (i.e., Yeatman et al., 2011). Further, it is possible to assess the volume of the tract by counting the number of voxels that it covers. In probabilistic tractography, it is common to estimate the probability that a certain voxel is connected to another via tract-density measures at the individual or group level. The estimated volumes, no matter how calculated, do not provide a direct measure of the number of axon projections or the connection strength between the connected regions (Jones, Knösche, & Turner, 2013).

Pathways implicated in tractography studies of PDS

Several studies have used tractography to detect differences in white matter pathways in people who stutter. Here, we review the consistent findings in the literature. Table 1 lists the main characteristics of the papers that used tractography to study PDS at the time of writing; Fig. 2 presents the most-replicated tracts. Other tracts, particularly ones featured in a single study, have been left out for the sake of generality and clarity.

The arcuate fasciculus (AF), a major long-range pathway that connects the inferior frontal cortex with the middle/inferior

Table 1
Studies that use tractography to investigate white matter properties in people who stutter (as of May 2nd, 2016).[a,b]

Study	Sample	Diffusion model	Tractography algorithm	Extracted measures	Targeted tracts	Most implicated pathways
Chang, Horwitz, Ostuni, Reynolds, and Ludlow (2011)	15 AWS 14 CON	Tensor Ball and stick	Probabilistic	Tract density in target regions	IFG to motor, premotor and STG cortices. VLN to motor and premotor cortices.	L IFG to L motor and premotor cortices (AWS < CON)
Chang and Zhu (2013)	27 CWS; 28 CON	2 Tensors Ball and stick	Probabilistic	Tract density in brain voxels	Auditory-motor and BG networks	LBG to motor and auditory cortices (AWS < CON)
Cai et al. (2014)	20 AWS; 18 CON	2 Tensors Ball and stick	Probabilistic	Tract density in target regions, network properties (graph theory)	Wide view of L and R speech networks	L speech network (AWS < CON)
Connally, Ward, Howell, and Watkins (2014)	29 CWS/ AWS; 37 CON	2 Tensors Ball and stick	Probabilistic	Tract volume, tract FA, number of streamlines	L and R AF L and R CST	L and R AF (AWS < CON in FA) CST (atypical asymmetry in FA)
Cieslak, Ingham, Ingham, and Grafton (2015)	8 AWS; 8 CON	Spectrum	Deterministic	Tract volume	whole-brain networks	L and R AF (AWS < CON) L BG to temporal regions (AWS > CON)
Kronfeld-Duenias et al. (2016a)	15 AWS; 19 CON	Tensor	Deterministic	Tract volume, Tract and profile analysis of FA, MD, AD, RD	L and R $AF_{ant,}$ L and R AF_{long} L and R IFOF L and R UF	L AF_{ant} and L AF_{long} (AWS < CON in volume) R AF_{ant} (AWS < CON in FA and AD; AWS > CON in RD)
Kronfeld-Duenias, Amir, Ezrati-Vinacour, Civier, and Ben-Shachar (2016b)	15 AWS; 19 CON	Tensor	Deterministic	Tract volume, Tract and profile analysis of FA, MD, AD, RD	L and R FAT L and R CST	L and R FAT (AWS > CON in MD, AD, RD) L CST (AWS > CON in MD)

[a] The studies are sorted by year of publication, then by author.

[b] Abbreviations: adults who stutter (AWS), children who stutter (CWS), controls (CON), fractional anisotropy (FA), mean diffusivity (MD), axial diffusivity (AD), radial diffusivity (RD), left (L), right (R), inferior frontal gyrus (IFG), superior temporal gyrus (STG), ventral lateral nucleus (VLN), basal ganglia (BG), arcuate fasciculus (AF), frontal aslant tract (FAT), corticospinal tract (CST), anterior segment of the arcuate fasciculus (AF_{ant}), long segment of the arcuate fasciculus (AF_{long}), inferior fronto-occipital fasciculus (IFOF), uncinate fasciculus (UF).

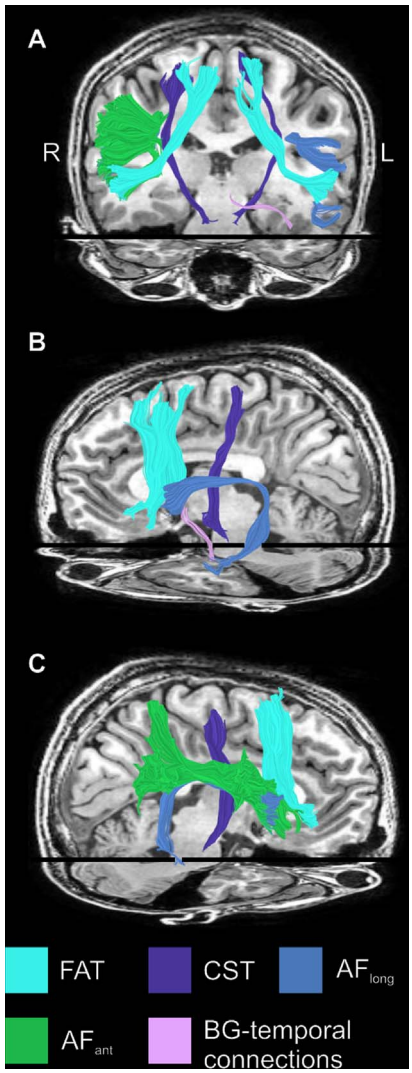

Fig. 2. Roadmap of the major white matter pathways indicated by tractography studies in people who stutter. The segmented tracts of a single participant (male, AWS, 24Y) are shown against T1 anatomical images of the same participant, viewed from the front (A), left (B) and right (C). The visible tracts are: the bilateral AF_{long} (light blue), bilateral FAT (cyan), bilateral CST (purple), right AF_{ant} (green) and the connections between the left BG nuclei and the cortex (shown are connections between the left nucleus accumbens and the inferior temporal lobe, following Cieslak et al., 2015, in pink) *Abbreviations*: long segment of the arcuate fasciculus (AF_{long}), frontal aslant tract (FAT), corticospinal tract (CST), anterior segment of the arcuate fasciculus (AF_{ant}), basal-ganglia (BG). For interpretation of the references to color in this figure legend, the reader is referred to the web version of this article.

temporal cortex[4] is most often implicated in tractography studies of PDS. Volume reductions have been reported in the left AF of adults who stutter (AWS) (Chang et al., 2011; Cieslak et al., 2015; Kronfeld-Duenias et al., 2016a) and in one case also in the right AF (Cieslak et al., 2015). FA reductions were reported in bilateral AF of individuals who stutter compared with controls (Connally et al., 2014). In one case, similar reductions were observed in the right anterior (fronto-parietal) segment of the AF (AF_{ant}) (Kronfeld-Duenias et al., 2016a).

A second tract implicated in PDS is the CST, a well-known component of the motor network that connects the primary motor and premotor cortices with the brain stem, cerebellum and spinal cord. Atypical asymmetry patterns in FA values were measured in the CST of young AWS, with individuals who stutter demonstrating lower FA in the left CST compared to the right CST (Connally et al.,

[4] The AF partially overlaps with the superior longitudinal fasciculus (SLF), therefore many studies use the terms AF and SLF interchangeably. Here, we use the term AF to refer to the fronto-temporal connections in general (including both the direct connections and connections that run through the parietal lobe). Whenever possible, we follow the more precise terminology suggested by Catani, Jones, and Ffytche (2005) that refers to different segments of the AF: the fronto-parietal 'anterior' segment (AF_{ant}), the parieto-temporal 'posterior' segment (AF_{post}) and the fronto-temporal 'long' segment (AF_{long}).

2014). MD elevations were also reported in a sub-region of the left CST of AWS (Kronfeld-Duenias et al., 2016b). This pattern of reduced FA and increased MD suggests less restricted and less directional diffusion in the CST of AWS compared with controls, which is consistent with either reduced myelination or fewer but thicker fibers in the CST of AWS.

Differences in the AF and in the CST, particularly in the left hemisphere, have already been suggested based on earlier voxel-based DTI studies (e.g., Chang et al., 2008; Watkins et al., 2008, among others). A third tract of interest that was only recently introduced to the literature is the frontal aslant tract (FAT). The FAT is a newly identified tract that connects the IFG with supplementary and pre-supplementary motor areas (Catani et al., 2013). Recent frameworks of the neurobiology of language suggest that the FAT is part of a "motor stream" in language (Dick, Bernal, & Tremblay, 2013) that complements the accepted dorsal and ventral language streams (Hickok & Poeppel, 2004, 2007). Elevated MD values were reported in the bilateral FAT of stuttering individuals, with MD values of the left tract demonstrating association with speech fluency (Kronfeld-Duenias et al., 2016b). To the best of our knowledge, the FAT has only been targeted by one study in PDS, however, the involvement of the left FAT in stuttering recently gained support from a stimulation study that demonstrated stuttering-like behaviors in non-stuttering patients who underwent awake electrical stimulation of the left FAT (Kemerdere et al., 2016).

Finally, tracts that connect the left basal ganglia have also been shown to differ between people who do and do not stutter using tractography. Recent studies indicate that pathways that project to the left putamen and reach the inferior frontal gyrus, middle temporal gyrus or supplementary motor area (among other locations) differ in children who stutter compared with controls (Chang & Zhu, 2013). Further, greater volume of the connections between the left ventral striatum and the left inferior temporal gyrus was reported in AWS compared with controls (Cieslak et al., 2015). Given these recent findings and earlier theories of the involvement of the basal ganglia in PDS (Alm, 2004), we expect that comparing the diffusion properties in cortical – basal ganglia circuits segmented in individual participants who stutter could provide valuable information about the involvement of these tracts in the disorder. While these networks are highly complex, the feasibility of their identification in humans has been well established (Draganski et al., 2008; Lehéricy, Ducros, De Moortele et al., 2004; Lehéricy, Ducros, Krainik, et al., 2004).

Taken together, the findings described above indicate PDS-related differences in the bilateral AF, CST, FAT and the connections between the left basal ganglia nuclei and the frontal and temporal lobes. Importantly, most tractography studies of PDS have used hypothesis-driven approaches by targeting pre-defined tracts of interest and comparing properties of those tracts between the groups (see Table 1). This approach is advantageous because it enhances sensitivity and interpretability of scientific discoveries. However, it might also bias the literature by over-studying some pathways and missing out on less expected strong effects (see 'Tractography vs. voxel-based analyses' in the discussion section). Three published studies performed large scale network-level analysis of the white matter pathways in PDS (Cai, et al., 2014; Cieslak, et al., 2015; Sitek, et al., 2016). One of those studies (Cieslak, et al., 2015) reported differences in the AF and in basal-ganglia connections that were also indicated by studies that pre-targeted these connections (e.g., Chang & Zhu, 2013; Connally, et al., 2014). A second study reported a general bias for reduced tract-densities in the left speech network of AWS compared with controls (Cai, et al., 2014); PDS-related differences were detected in tract-densities of multiple connections in this latter study, but those were difficult to integrate into the common nomenclature of white matter pathways because the connections were listed based on their cortical endpoints, without specifying their trajectory. For example, reduced tract density in multiple connections of the left SMA highlights the importance of the left SMA in PDS but does not specify affected white matter pathways (see Fig. 6 of Cai et al., 2014). Using a similar approach, a third study (Sitek et al., 2016) indicated differences in structural connectivity of widespread networks in PDS.[5] In terms of the implicated pathways, this latter study showed differences in the volume and FA measures of the right posterior (temporo-parietal) portion of the arcuate fasciculus (AF_{post}), the posterior callosum and the left uncinate fasciculus.

Wide-lens analysis: motivation

Voxel-based analyses of the diffusion data provide a comprehensive, wide-coverage tool to detect regions of robust group-differences (or within-group neurobehavioral associations). Such tools may detect differences (or correlations) across the entire brain, potentially shifting the scientific attention to regions that were not assessed in hypothesis-driven studies. However, these methods are limited by registration errors, potentially resulting in different pathways from different participants registering to a single voxel in template space. This risk is enhanced when there are known volumetric differences between the study- and control- population. Additionally, voxel-based methods are limited in their ability to map a difference in a cluster of voxels in template space to affected pathways in individual brains (as was discussed earlier in the case of the left RO).

Tractography studies, on the other hand, can be performed in the native space of single individuals, which makes them less susceptible to inter-subject registration errors. These methods provide valuable information about the targeted pathways, allowing the detection of subtle group-differences and individual brain-behavior associations. Unfortunately, tractography methods typically rely on manual definition of individual regions of interest and manual cleaning of the resulting fibers. This introduces issues of reliability and in many cases, results in the study of a limited number of pathways based on prior hypotheses (but see Cai et al., 2014; Cieslak et al., 2015; Sitek et al., 2016 in PDS). While this approach has been very productive and enhances the interpretability of findings, it has the potential to create a bias towards over-studying certain pathways and over-looking others ('a streetlight effect').

Here, we use a third approach that combines wide-coverage and objectivity with the sensitivity of tractography-based

[5] The paper by Sitek et al. (2016) was not available at the time of the literature review (May 2nd, 2016). Therefore, it is not referenced in Table 1. We still refer to this paper here, because of its relevance to the topic.

individualized methods. Using an automated procedure, we segment multiple cortico-cortical white matter bundles in the native space of individual participants, and quantify the diffusivity properties of each of these tracts in each individual. Using this approach, we attempt to (1) replicate earlier findings in the AF, CST and in the corpus callosum and (2) provide new insights about the potential role of other cortico-cortical tracts that may have been missed out by earlier tractography studies. Given the exploratory nature of this approach, any novel findings that may arise here will generate new hypotheses that can be tested in future targeted studies.

Methods

We compared diffusion measurements along 18 major white matter pathways (Wakana et al., 2007) in a sample of 25 AWS and 19 controls. Tracts were segmented in each participant's brain, and diffusion properties were extracted from these tracts and compared between the groups.

Participants

A total of 44 individuals participated in this study. The participants were all native Hebrew speakers. They were physically healthy and reported no history of neurological disease or psychiatric disorder. Before participating, each participant signed a written informed consent according to protocols approved by the Helsinki committee of the Tel-Aviv Sourasky Medical Center and by the Ethics committee of the Humanities Faculty in Bar Ilan University. Data from a sub-sample of 34 participants have been included in other published analyses (Civier et al., 2015; Kronfeld-Duenias et al., 2016a, 2016b). The inclusion criteria and the assessment of stuttering frequency are reported in detail in two of these prior publications (see Kronfeld-Duenias et al., 2016b).

Twenty-five participants were assigned to the group of AWS (mean age: 31 y, age range [19 y–52 y], six females) and 19 participants were assigned to the control group (mean age: 33y, age range [19 y–53 y], three females). For each participant, we calculated the percent of stuttering like disfluencies (SLD; Ambrose & Yairi, 1999) and the overall percent of stuttered syllables. In AWS, we further valuated the stuttering severity scores using the Stutteing Severity Instrument (SSI-III; Riley, 1994). Table 2 presents the average demographic characteristics and the assessment of stuttering frequency in AWS and in control participants.

Participants in the group of AWS scored an average SSI score of 24.42 (standard deviation: 8.5; range [10–41.5]). The wide range of SSI scores indicates that this group exhibited different degrees of symptoms, ranging from very mild to very severe. The clinical evaluation of speech fluency measures verified a significant group difference between AWS and fluent controls in both measures of speech fluency (SLD: $t(42) = 2.98$, $p < 0.05$; percent of stuttered syllables: $t(42) = 3.64$, $p < 0.001$). The groups did not differ in age, handedness or education levels (see Table 2).

Image acquisition and data preprocessing

Magnetic resonance imaging (MRI) was performed on a 3T General Electric MRI scanner at the Tel-Aviv Sourasky Medical Center. The MRI acquisition protocol and the data preprocessing were described in length in earlier publications of our group (e.g., Kronfeld-Duenias et al., 2016b). For clarity, we briefly iterate the main parameters used during the acquisition of the dMRI data. Using a standard diffusion tensor imaging (DTI) protocol applied by means of a single-shot spin-echo diffusion-weighted echo-planar imaging (DW-EPI) sequence, we collected ~68 axial slices, adjusting the number of slices to cover the entire cerebrum in each participant (FOV = 240 mm; 128 × 128 matrix; 2 mm thick axial slices; voxel size: ~2 × 2 × 2 mm). 19 diffusion-weighted volumes ($b = 1000$ s/mm^2) and one reference volume ($b = 0$ s/mm^2) were acquired using a standard direction matrix.

Table 2
Subject demographics and fluency measures.[a]

	AWS (n = 25)	*controls (n = 19)*	*P*
Age (years)	30.72 (8.59)	33.26 (9.91)	n.s
Gender	19 M/6F	16 M/3F	n.s
Handedness[b]	95 (8.85)[c]	89.63 (17.84)	n.s
Education (years)	14.57 (3.3)[d]	15.31 (2.8)	n.s
SLD (%)	14.3 (17.63)	2.18 (1.04)	P = 0.005**
St. Syll. (%)	9.78 (9.12)	2.1 (1.0)	P = 0.0007**

Abbreviations;: adults who stutter (AWS), stuttering-like-disfluencies (SLD) per 100 syllables, stuttered syllables (St. Syll.), not significant (n.s), male (M), female (F).

[a] Mean values and standard deviations (in parentheses) are shown for AWS and control participants.

[b] Handedness scores are based on the Edinburgh handedness inventory (Oldfield, 1971). 100 indicate full right handedness, −100 indicate full left handedness.

[c] Handedness data is missing in one AWS (N = 24).

[d] Education data is missing in two AWS (N = 23).

** $p < 0.01$.

Tract segmentation and quantification

Tractography was performed with AFQ, an open-source package of MATLAB functions designed for automated segmentation and quantification of major fiber tracts (Yeatman, Dougherty, Myall, Wandell, & Feldman, 2012). Briefly explained, AFQ consists of three stages: (1) whole-brain tractography, (2) automatic tract segmentation and (3) tract quantification. Whole-brain tractography was performed using a deterministic streamlines tracking algorithm (STT; Basser, Pajevic, Pierpaoli, Duda, & Aldroubi, 2000; Mori, Crain, Chacko, & Van Zijl, 1999), with a fourth-order Runge-Kutta path integration method. The tracking algorithm was seeded with a white matter mask including all voxels with FA greater than 0.2 (e.g., Travis, Adams, Ben-Shachar, & Feldman, 2015; Yeatman, et al., 2011). Tracking was halted when FA dropped below 0.15, because such values in adults are typical of gray matter or CSF, not white matter (Bhagat & Beaulieu, 2004; Pierpaoli & Basser,1996) and, thus, following the principal diffusion direction in these voxels is unlikely to produce reliable fibers. Tracking was also ceased if the angle between the last and the next step direction was greater than 30° (Dougherty, et al., 2007). The minimum virtual-fiber length was set to 20 mm while the maximum length was set to 500 mm.

Tract segmentation was achieved using a two-waypoint region of interest (ROI) procedure as defined by Wakana et al. (2007). First, an estimated non-linear transformation was applied to automatically warp predefined ROIs from the Montreal Neurological Institute (MNI) template into each individual's native space. Then, the fibers tracked from the entire brain were intersected with the individual ROIs using logical AND operations, to segment tracts that pass through both ROIs. The resulting tracts were cleaned automatically using a statistical outlier rejection algorithm that removed fibers more than 4 standard deviations above the mean fiber length or that deviate more than 5 standard deviations in distance from the core of the fiber tract (Yeatman, et al., 2012).

Using this procedure, we isolated 18 major pathways for each participant in the participant's native space: The posterior and anterior segments of the corpus callosum (i.e., the forceps major and forceps minor, FMajor and FMinor, respectively) and eight pairs of bilateral pathways, including the anterior thalamic radiations (ATR), the cingulum (Cing), the corticospinal tract (CST), the inferior fronto-occipital fasciculus (IFOF), the inferior longitudinal fasciculus (ILF), the uncinate fasciculus (UF) the anterior segment of the arcuate fasciculus (AF_{ant}) and the long segment of the arcuate fasciculus (AF_{long}). The left hemisphere tracts segmented in a single participant of the stuttering group are shown in Fig. 3.

Tracts were quantified at two levels. First, we calculated the average FA and average MD across all voxels visited by the tract. These summary measures are termed *tract-FA* and *tract-MD*, respectively. To further identify the tract location that differ between the groups, we calculated *tract profiles* by sampling each tract at 100 equi-spaced nodes along the length of the tract (between the two ROIs used for its definition), and calculating FA and MD in each node as a weighted average of nearby tract fibers (for details, see Yeatman et al., 2012). Both tract-FA, tract-MD, and their respective tract profiles were calculated for each individual separately, and later subject to group statistics as described in the following subsection.

Statistical analyses

To assess group differences in tract properties, we first calculated two-tailed *t*-tests for independent measures on the tract-FA and tract-MD of each tract. To account for multiple comparisons across 18 tracts, we controlled for the false discovery rate (FDR; Benjamini & Hochberg, 1995) with a corrected alpha level set to 0.05. In tracts that showed a significant group difference in tract-FA or tract-MD, we further compared FA and MD profiles between the groups using multiple two-tailed *t*-tests for independent samples at each node along the tract. Significance was corrected to account for multiple comparisons (number of tracts X 100 nodes in each tract). To this end, we used a family-wise error (FWE) permutation-based correction method (Nichols & Holmes, 2001), setting the corrected alpha to 0.05. This method produces a critical cluster size which is then applied to clusters of adjacent nodes along the tract profile. Clusters of adjacent nodes that show significant (uncorrected) *t*-tests between the groups are considered significant (corrected) only if the cluster size is larger than the critical cluster size.

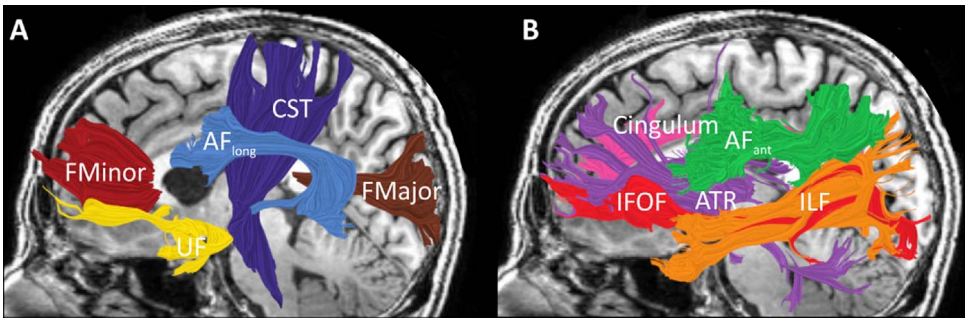

Fig. 3. Tractography of major cerebral white matter tracts. Eight tracts of the left hemisphere and two callosal segments are visualized in a single participant (male, AWS, 35Y) against the background of his sagittal T1 images. The right hemisphere tracts were also segmented in each participant, but they are not visualized here. Panel A illustrates the long segment of the arcuate fasciculus (AF_{long}; light blue), corticospinal tract (CST; purple), forceps minor (FMinor; dark red), forceps major (FMajor; brown) and the uncinate fasciculus (UF; yellow). Panel B illustrates the anterior thalamic radiation (ATR; purple), cingulum (magenta); inferior fronto-occipital Fasciculus (IFOF; red), inferior longitudinal fasciculus (ILF; orange) and the anterior segment of the arcuate fasciculus (AF_{ant}; green). For interpretation of the references to color in this figure legend, the reader is referred to the web version of this article.

Finally, two follow-up statistical analyses were performed. First, to assess the effect of age on the results, tract-FA and tract-MD were entered into two separate mixed-design analyses of covariance (ANCOVAs) with Group (PDS/controls) as a between-subject factor, Tract as a within-subject factor, and Age as a covariate of no interest. Degrees of freedom were corrected using Greenhouse-Geisser estimates in cases where sphericity was violated (Mauchly, 1940). Measures of speech fluency were not included as covariates in these ANCOVAs because such measures are inherently different between the groups. Therefore, removing the contribution of these measures is likely to wipe out the variability that is of interest in this study. A second complementary analysis addressed the possibility of non-specific group differences in diffusivity. To this end, tract-FA (and tract-MD) values were normalized relative to the mean FA (or MD) of the whole-brain tractography, while taking into account the variability of FA (or MD) values across the whole-brain tractography. Normalized measures were then compared between the groups. The normalized tract-FA and tract-MD scores for tract j of participant i were calculated as follows:

$$normalizedTractFA_{i,j} = \frac{meanFA_{i,j} - meanFA_{i,wholeBrainFg}}{stdFA_{i,wholeBrainFg}}$$

$$normalizedTractMD_{i,j} = \frac{meanMD_{i,j} - meanMD_{i,wholeBrainFg}}{stdMD_{i,wholeBrainFg}}$$

where $meanFA_{i,j}$ is the average of FA values in all voxels covered by tract j of participant i (in other words, tract-FA of tract j in participant i). $MeanFA_{i,wholeBrainFg}$ and $StdFA_{i,wholeBrainFg}$ are the average and standard deviation (respectively) of FA values in voxels covered by the whole-brain tractography of participant i. Similarly, $meanMD_{i,j}$ is the average of MD values in all voxels covered by tract j of participant i (tract-MD of tract j of participant i). $MeanMD_{i,wholeBrainFg}$ and $StdMD_{i,wholeBrainFg}$ are the mean and standard deviation (respectively) of MD values in voxels covered by the whole-brain tractography of participant i. The normalized values were compared between the groups using two-tailed *t*-tests for independent measures while controling the FDR.

Software

Data preprocessing was performed using the 'mrDiffusion' package (http://web.stanford.edu/group/vista/cgi-bin/wiki/index.php/MrDiffusion) and functions from SPM5 (Friston & Ashburner, 2004) using MATLAB 2012b (The Mathworks, Nattick, MA). Tract segmentation and quantification was performed with the AFQ package (Yeatman, et al., 2012). Visual inspection of the tracts was performed with Quench (Akers, 2006). Statistical analyses were conducted using SPSS Version 21 (IBM Corp, Armonk, NY).

Results

Eighteen major pathways have been segmented in each participant, as demonstrated in Fig. 3. AWS showed a significant reduction in tract-FA of the right ILF compared with controls ($t(42) = 3.34$, $p < 0.05$, FDR corrected). Tract-FA reductions were also observed in AWS in the right cingulum and the forceps minor ($t(42) = 2.44$; $t(42) = 2.02$, $p < 0.05$, uncorrected) but these effects did not survive FDR correction (see Fig. 4). Conceivably, averaging FA values across the entire tract may mask out significant, but local, group differences. We therefore followed up on all three tracts with a more sensitive, FA profile analysis that compares group FA values in multiple positions along the tract.

The FA profile analysis revealed large clusters of nodes that differed between the groups within the right ILF and the right cingulum. In both tracts, FA was significantly reduced in AWS compared with controls. In the right ILF, two large clusters of nodes with reduced FA were identified (Fig. 5A, nodes 29–53 and nodes 57–83, $p < 0.05$, FWE corrected across 3×100 nodes). In the

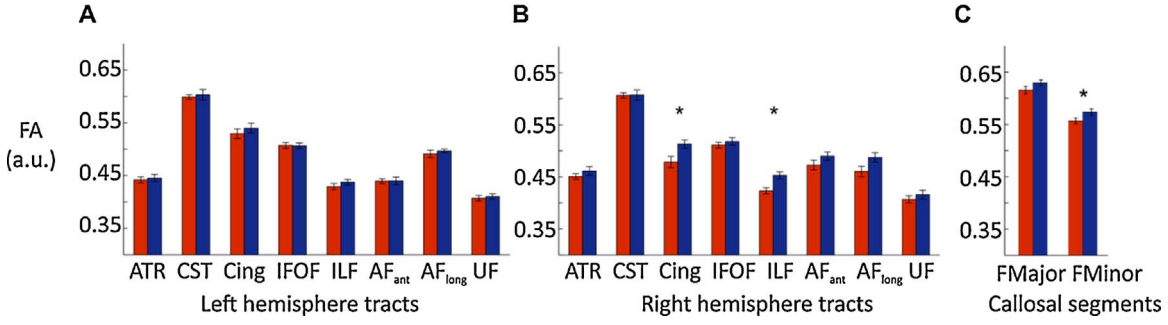

Fig. 4. Group comparison of tract-FA values. The group-average FA values are shown in the left hemisphere tracts (A), right hemisphere tracts (B) and in the callosal segments (C) of AWS (red) and controls (blue), with error bars representing ± 1 standard error of the mean. Significant group differences are marked with asterisk ($p < 0.05$). Reduced FA in AWS compared with controls is observed in two right hemisphere tracts: the right ILF ($p < 0.05$, FDR corrected) and the right cingulum ($p < 0.05$, uncorrected), as well as in the anterior callosum (FMinor, $p < 0.05$, uncorrected). No significant difference is found in any of the left hemisphere tracts. *Abbreviations:* fractional anisotropy (FA), arbitrary units (a.u.) anterior thalamic radiation (ATR), corticospinal tract (CST), cingulum (Cing), inferior fronto-occipital fasciculus (IFOF), inferior longitudinal fasciculus (ILF), anterior segment of the arcuate fasciculus (AF_{ant}), long segment of the arcuate fasciculus (AF_{long}), uncinate fasciculus (UF), forceps major (FMajor), forceps minor (FMinor). For interpretation of the references to color in this figure legend, the reader is referred to the web version of this article.

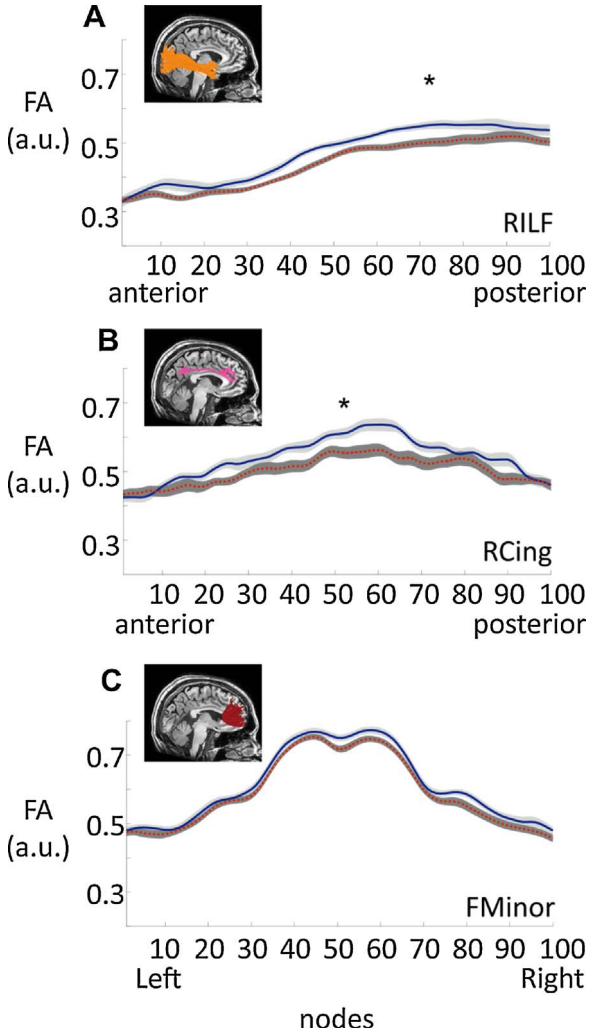

Fig. 5. Group comparison of FA profiles. FA profiles of the RILF (A), RCing (B), and FMinor (D) are shown in AWS (red) and in controls (blue). The colored lines indicate the average group FA profiles with gray regions denoting ± 1 standard error of the mean (AWS: dark gray; controls: light gray). The profiles were calculated between the ROIs used for tract segmentation. Significant group differences (marked with an asterisk) are found in the RILF (nodes 29–53 and 57–83, $p < 0.05$, FWE corrected) and in the RCing (nodes 37–67, $p < 0.05$, FWE corrected). The insets at the top left of each panel demonstrate the relevant tracts in a single participant. *Abbreviations*: fractional anisotropy (FA), arbitrary units (a.u.), right inferior longitudinal fasciculus (RILF), right cingulum (RCing), forceps minor (FMinor). For interpretation of the references to color in this figure legend, the reader is referred to the web version of this article.

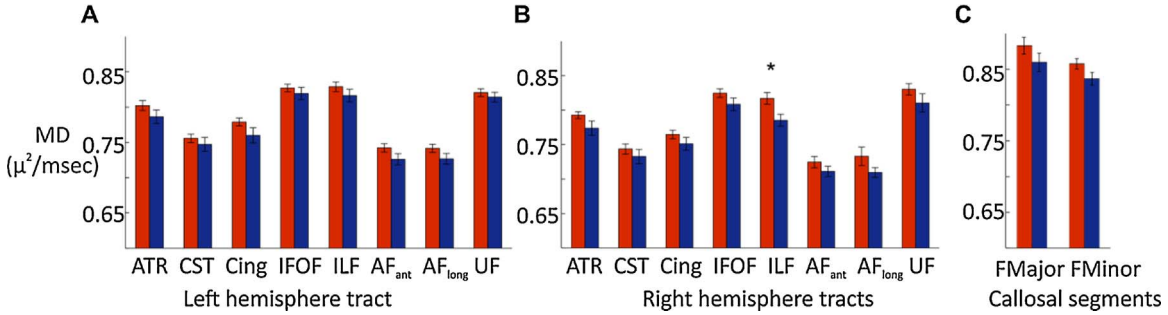

Fig. 6. Group comparison of tract-MD values. The group-average MD values are shown in the left hemisphere tracts (A), right hemisphere tracts (B) and in the callosal segments (C) of AWS (red) and controls (blue), with error bars representing ± 1 standard error of the mean. Increased MD is observed in the right ILF of AWS compared with controls ($p < 0.05$, uncorrected). *Abbreviations*: mean diffusivity (MD), the rest as in Fig. 4. For interpretation of the references to color in this figure legend, the reader is referred to the web version of this article.

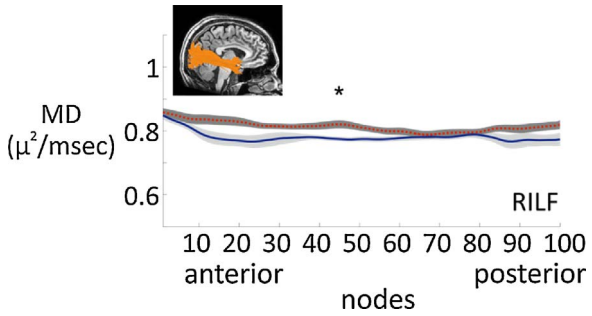

Fig. 7. Group comparison of MD profiles. MD profiles of the RILF are shown in AWS (red) and controls (blue). The colored lines indicate the average profiles of the different groups, with gray regions denoting ± 1 standard error of the mean (AWS: dark gray; controls: light gray). The profiles were calculated between the ROIs used for tract segmentation. Significant group differences are found in nodes 33–55 (marked with an asterisk, $p < 0.05$, FWE corrected). The inset at the top left corner demonstrates the right ILF in a single participant. *Abbreviations*: mean diffusivity (MD), right inferior longitudinal fasciculus (RILF). For interpretation of the references to color in this figure legend, the reader is referred to the web version of this article.

right cingulum, a single large cluster of 30 nodes differed significantly between the groups (Fig. 5B, nodes 37–67, $p < 0.05$, FWE corrected across 3 × 100 nodes). In the forceps minor, we did not find any cluster of nodes that differed significantly between the groups and was large enough to survive the multiple comparison cluster-based threshold (Fig. 5c), indicating that in this tract the differences were more wide-spread and could not be localized in specific clusters.

AWS showed a significant elevation in tract-MD of the right ILF compared with controls (Fig. 6, $t(42) = 2.55$, $p < 0.05$, uncorrected). We followed up on this finding with an MD profile analysis that compared group MD values in multiple positions along the tract, as was done in the case of FA. This analysis revealed a significant cluster of nodes within the right ILF where MD values were elevated in AWS compared with controls (Fig. 7, nodes 33–55, $p < 0.05$, FWE corrected across 1 × 100 nodes).

To evaluate the potential contribution of age to the results, we conducted mixed design ANCOVAs on tract-FA and tract-MD values, with group as between subject variable, tract as within subject variable, and age as covariate. Both ANCOVAs revealed main effects of Group (tract-FA: $F = 4.53$, $p < 0.05$; tract-MD: $F = 4.81$, $p < 0.05$) that suggest that the groups differed in FA and MD over and above the effect of age. Significant main effects of Tract were also evident (tract-FA: $F = 22.148$, $p < 0.0001$; tract-MD: $F = 10.1$, $p < 0.0001$), indicating that tracts vary in overall FA and MD, again, over and above the effect of age. Importantly, the ANCOVAs revealed no significant main effects of Age (tract-FA: $F = 3.83$, $p > 0.05$; tract-MD: $F = 1.765$, $p > 0.1$) and no significant Tract by Age interaction (tract-FA: $F = 0.94$, $p > 0.4$; tract-MD: $F = 1.448$, $p > 0.1$), suggesting that the Age factor did not have a significant contribution to the results.

Last, to evaluate the specificity of our findings, the original analysis was repeated on normalized tract-FA and normalized tract-MD values (see Methods). The results showed a significant group-difference in normalized tract-FA of the right ILF ($p < 0.05$, corrected), and trends for group differences in normalized tract-FA of the right cingulum ($p < 0.05$, uncorrected) and in normalized tract-MD of the right ILF ($p < 0.05$, uncorrected). These results resemble the original findings (without normalization), suggesting that the effect in these tracts cannot be explained by an overall group-difference.

Discussion

Previous tractography studies of PDS have detected atypical diffusion properties in multiple white matter pathways, including the long and anterior segments of the arcuate fasciculus, the corticospinal tracts, the frontal aslant tracts and cortico-basal ganglia connections. Using an automated large scale tractography approach we identify additional white matter pathways that may play a role in PDS. Specifically, we show that, in the current sample, diffusion properties of the right ILF and the right cingulum differ between AWS and fluent controls.

Our tractography findings in light of the literature

The ILF is a major pathway connecting the posterior occipito-temporal regions with the middle and inferior temporal pole, parahippocampal gyrus and the amygdala (Catani, Jones, & Donato, 2003). Functionally, the ILF was proposed as part of an “indirect” ventral semantic stream, however, its' role in semantic language processing was reported “not indispensable” (Duffau, Moritz-Gasser, & Mandonnet, 2014; Mandonnet, Nouet, Gatignol, Capelle, & Duffau, 2007). While most of the empirical data on the functional role of this tract come from the left hemisphere, few studies identified the right ILF (implicated in this study) and reported that it is involved in visual object recognition (Ortibus, et al., 2012; Tavor, et al., 2014). Microstructural differences in the right ILF were previously reported in children who stutter (Chang, et al., 2008) using voxel-based analysis, however, these differences were in the opposite direction to the FA reduction that we report here in adults, suggesting a potential developmental cross-over effect. Given the novelty of our finding in the right ILF, future studies that target the right ILF in PDS will be essential to establish the stability of this finding across different cohorts.

The cingulum is a major limbic pathway that consists of a compact bundle of long and short association fibers connecting the

cingulate cortex with the parahippocampal gyrus, medial prefrontal cortex, and medial cortical regions in the parietal and occipital lobes (Mori & Aggarwal, 2014; Schmahmann, et al., 2007). Microstructural properties of the cingulum were associated with the ability to infer intentions (Herbet, et al., 2014) and regulate attention to negative interpersonal stimuli (Keedwell, et al., 2016). PDS-related group differences in the cingulum may be associated with the role of emotional social-related processing in this disorder. This possibility still remains to be tested via correlational analyses that will assess the relation between emotional or social variables and the microstructural properties of the cingulum in individuals who stutter.

An interesting question with regards to emotional processing in PDS is whether or not people who stutter can be characterized by certain personality traits, and if so, what comes first (i.e., stuttering or the specific personality traits that accompany it). A recent review that addressed this question in children concluded against the group-characterization of children who stutter as children who have a tendency towards shyness and social anxiety (Alm, 2014). According to the latter report, the elevated levels of anxiety and negative mood states, that are often observed in people who stutter, develop with time and are confined to social situations that involve speech. A recent voxel-based DTI study in children who stutter showed a significant Group by Age interaction in FA values measured in the right cingulum (Chang, et al., 2015), with controls exhibiting greater FA increases with Age compared to children who stutter. Assuming that FA of the right cingulum is indeed related to emotional processing in PDS, our study and this latter study may be taken as a neuroanatomical support to the hypothesis that PDS-related personality traits develop following years of stuttering. Longitudinal measurements in children who stutter will be necessary in order to test this hypothesis directly. If it is correct, we expect differences in the microstructural properties of the right cingulum to emerge over time, in correlation with the rate of change in emotional variables measured in the same set of participants. The current study did not assess emotional variables even cross-sectionally, so we cannot evaluate associations between emotional processing and microstructural properties of the cingulum in our sample.

Our wide-lens analysis replicates earlier findings of FA reductions in the callosum of individuals who stutter (Cai et al., 2014; Chang et al., 2015; Civier et al., 2015; Connally et al., 2014; Cykowski et al., 2010; Kell et al., 2009). Interestingly, earlier studies vary with regards to the specific location of the group difference, with differences found in the anterior callosum (Cai et al., 2014; Civier et al., 2015; Cykowski et al., 2010; Kell et al., 2009) or in the posterior callosum (Chang et al., 2015; Connally et al., 2014; Neef et al., 2015). Our study converges with the former types of findings, but there is still room for a systematic investigation of the exact location of callosal differences in PDS as a function of age, stuttering severity, intervention history and more.

To our surprise, our analysis did not detect group differences in the long and anterior segments of the arcuate fasciculus, nor in the corticospinal tracts. These tracts were identified in earlier tractography studies of PDS (including ours), and match well-known effects at the voxel level, yet they did not show up in the current sample and analysis. Failing to replicate earlier findings in a single sample does not entail their disqualification, however, it deserves an explanation. We suggest that the discrepancy between our findings and earlier findings may represent the shortcoming of a wide-lens approach, in comparison to a hypothesis based approach that zooms in on a few pre-selected tracts. The former has the potential of discovering new and unexpected strong effects in the data. However, it is also prone to miss weaker, but replicable, localized effects. In addition, sample-specific characteristics may explain some of the variability and contradicting patterns of results in the emerging tractography literature in PDS. As in any other developmental clinical population, individual differences in personal traits, compensatory strategies and other intervening factors may play a prominent role in determining group differences, and those are yet to be explored in relation to white matter properties. We expect that the next decade of dMRI research in PDS will lead to better understanding of the relation between tract properties and the clinical profiles of individuals who stutter.

Group differences detected here, combined with prior findings, suggest the involvement of both hemispheres in PDS. This bilateral pattern of findings fits well with prior findings from functional imaging studies (Belyk et al., 2015; Biermann-Ruben, Salmelin, & Schnitzler, 2005; Chang, Kenney, Loucks, & Ludlow, 2009; Kell et al., 2009; Lu et al., 2010; Watkins et al., 2008; Xuan et al., 2012). It is also compatible with structural imaging studies that show atypicalities in the corpus callosum of individuals who stutter (Beal, Gracco, Brettschneider, Kroll, & De Nil, 2013; Cai et al., 2014; Choo, Chang, Zengin-Bolatkale, Ambrose, & Loucks, 2012; Choo et al., 2011; Civier et al., 2015; Cykowski et al., 2010). We show that our findings go beyond potential differences in whole-brain FA or MD (by repeating the analysis on normalized FA/MD values). Significant main effects of Group (across tract and age) detected in the ANCOVAs suggest that some across-the-board difference may exist in our samples of PDS and controls. While we cannot rule out the possibility of some group-related bias in data analysis, we consider this option less plausible considering that the entire analysis pipeline was carried out automatically in this study (i.e., without manual definition of ROIs or subjective cleaning of individual fibers). Such overall differences in FA or MD are more likely to represent a sample-specific attribute rather than a characteristic of the PDS population.

Inferring from tractography about the biological properties of the brain tissues

Diffusion based MRI and tractography in particular have allowed scientists to come a long way towards the assessment of white matter pathways in relation to function, in typical development and in disease. However, in some cases, researchers attempt to use tractography as a direct measure of brain connectivity. It is important to recall that tractography does not directly measure the *degree of connectivity* of the underlying tissue or the *connection strength* between regions (Jones, et al., 2013). Instead, tractography provides measures of diffusion that probe the microstructure of the underlying tissue. The interpretation of any measure obtained from dMRI data should, therefore, be handled with great caution. New, quantitative imaging sequences and analysis schemes provide complementary information that allow more direct assessment of biological properties such as myelin content (Mezer et al., 2013; Stikov et al., 2011), axonal diameter (Assaf, Blumenfeld-Katzir, Yovel, & Basser, 2008) and transmission speed (Horowitz et al., 2014).

Combined with tractography algorithms, such tools will allow more specific interpretation of group differences in terms of pathway properties in the foreseeable future.

Summary and conclusions

Persistent developmental stuttering is a complex disorder that mainly manifests in disrupted speech fluency. Tractography studies identify differences in multiple, bilateral, white matter pathways of individuals who stutter. The affected pathways encompass the bilateral arcuate fasciculus (including fronto-temporal and fronto-parietal connections), the corpus callosum, the frontal aslant tract, the corticospinal tract and cortical connections with the basal-ganglia. It is possible that these tracts are functionally involved in motor aspects of language processing. Our findings indicate that the right ILF and the right cingulum may also be affected in PDS, broadening the affected circuits beyond the left hemisphere and beyond known language and motor pathways.

Conflict of interest

The authors declare no competing financial interests.

Acknowledgments

This work is supported by the Israel Science Foundation [grant #513/11 awarded to M.B.-S and O.A], and by a Marie Curie International Reintegration Grant [DNLP 231029] awarded to M.B.-S. by the European Commission. V.K.D and O.C. were supported by the Israeli Center of Research Excellence in Cognition [I-CORE Program 51/11]. O.C. was supported by the Center for Absorption in Science, Ministry of Immigration Absorption, The state of Israel. We thank the Israeli Stuttering Association (AMBI) for help with participant recruitment. We also thank the team at the Wohl institute for advanced imaging in Tel Aviv Sourasky Medical Center, for assistance with protocol setup and MRI scanning. We are grateful to Tali Halag-Milo for her assistance in data acquisition and to Maya Yablonski for providing valuable insights at all stages of manuscript preparation.

References

Akers, D. (2006). CINCH: A cooperatively designed marking interface for 3D pathway selection. *User Interface Software and Technology meeting*.
Alexander, A. L., Hurley, S. A., Samsonov, A. A., Adluru, N., Hosseinbor, A. P., Mossahebi, P., et al. (2012). Characterization of cerebral white matter properties using quantitative magnetic resonance imaging stains. *Brain Connectivity, 1*, 423–446.
Alexander, A. L., Lee, J. E., Lazar, M., & Field, A. S. (2007). Diffusion tensor imaging of the brain. *Neurotherapeutics, 4*, 316–329.
Alm, P. A. (2004). Stuttering and the basal ganglia circuits: A critical review of possible relations. *Journal of Communication Disorders, 37*, 325–369.
Alm, P. A. (2014). Stuttering in relation to anxiety, temperament, and personality: Review and analysis with focus on causality. *Journal of fluency disorders, 40*, 5–21.
Ambrose, N. G., & Yairi, E. (1999). Normative disfluency data for early childhood stuttering. *Journal of Speech, Language, and Hearing Research, 42*, 895–909.
Assaf, Y., & Basser, P. J. (2005). Composite hindered and restricted model of diffusion (CHARMED) MR imaging of the human brain. *NeuroImage, 27*, 48–58.
Assaf, Y., Blumenfeld-Katzir, T., Yovel, Y., & Basser, P. J. (2008). AxCaliber: A method for measuring axon diameter distribution from diffusion MRI. *Magnetic Resonance in Medicine, 59*, 1347–1354.
Basser, P. J. (1995). Inferring macrostructural features and the physiological state of tissues from diffusion weighted images. *NMR in Biomedicine, 8*, 333–344.
Basser, P. J., Mattiello, J., & LeBihan, D. (1994). MR diffusion tensor spectro-scopy and imaging. *Biophysical Journal, 66*, 259–267.
Basser, P. J., Pajevic, S., Pierpaoli, C., Duda, J., & Aldroubi, A. (2000). In vivo fiber tractography using DT-MRI data. *Magnetic Resonance in Medicine, 44*, 625–632.
Basser, P. J., & Pierpaoli, S. (1996). Microstructural and physiological features of tissues elucidated by quantitative diffusion tensor MRI. *Journal of Magnetic Resonance, 111*, 209–219.
Beal, D. S., Gracco, V. L., Brettschneider, J., Kroll, R. M., & De Nil, L. F. (2013). A voxel-based morphometry (VBM) analysis of regional grey and white matter volume abnormalities within the speech production network of children who stutter. *Cortex, 49*, 2151–2161.
Behrens, T. E., Berg, H. J., Jbabdi, S., Rushworth, M., & Woolrich, M. (2007). Probabilistic diffusion tractography with multiple fibre orientations: What can we gain? *NeuroImage, 34*, 144–155.
Behrens, T. E., Woolrich, M. W., Jenkinson, M., Johansen-Berg, H., Nunes, R. G., Clare, S., et al. (2003). Charachterization and propagation of uncertainty in diffusion weigthed MR imaging. *Magnetic Resonance in Medicine, 50*, 1077–1088.
Belyk, M., Kraft, S. J., & Brown, S. (2015). Stuttering as a trait or state–An ALE meta-analysis of neuroimaging studies. *European Journal of Neuroscience, 41*, 275–284.
Ben-Shachar, M., Dougherty, R. F., & Wandell, B. A. (2007). White matter pathways in reading. *Current Opinion in Neurobiology, 17*, 258–270.
Benjamini, Y., & Hochberg, Y. (1995). Controlling the false discovery rate: A practical and powerful approach to multiple testing. *Journal of the Royal Statistical Society. Series B (Methodological), 57*, 289–300.
Bhagat, Y. A., & Beaulieu, C. (2004). Diffusion anisotropy in subcortical white matter and cortical gray matter: Changes with aging and the role of CSF-suppression. *Journal of Magnetic Resonance Imaging, 20*, 216–227.
Biermann-Ruben, K., Salmelin, R., & Schnitzler, A. (2005). Right Rolandic activation during speech perception in stutterers: A MEG study. *NeuroImage, 25*, 793–801.
Brown, S., Ingham, R. J., Ingham, J. C., Laird, A. R., & Fox, P. T. (2005). Stuttered and fluent speech production: An ALE meta-analysis of functional neuroimaging studies. *Human Brain Mapping, 25*, 105–117.
Buchanan, C. R., Pernet, C. R., Gorgolewski, K. J., Storkey, A. J., & Bastin, M. E. (2014). Test-retest reliability of structural brain networks from diffusion MRI. *NeuroImage, 86*, 231–243.
Budde, K. S., Barron, D. S., & Fox, P. T. (2015). Stuttering, induced fluency, and natural fluency: A hierarchical series of activation likelihood estimation meta-analyses. *Brain and Language, 139*, 99–107.
Cai, S., Tourville, J. A., Beal, D. S., Perkell, J. S., Guenther, F. H., & Ghosh, S. S. (2014). Diffusion imaging of cerebral white matter in persons who stutter: Evidence for network-level anomalies. *Frontiers in Human Neuroscience, 8*, 54.
Catani, M., Dell'Acqua, F., Vergani, F., Malik, F., Hodge, H., Roy, P., et al. (2012). Short frontal lobe connections of the human brain. *Cortex, 48*, 273–291.
Catani, M., Jones, D. K., & Donato, R. (2003). Occipito-temporal connections in the human brain. *Brain, 126*, 2093–2107.
Catani, M., Jones, D. K., & Ffytche, D. H. (2005). Perisylvian language networks of the human brain. *Annals of Neurology, 57*, 8–16.
Catani, M., Mesulam, M. M., Jakobsen, E., Malik, F., Martersteck, A., Wieneke, C., et al. (2013). A novel frontal pathway underlies verbal fluency in primary progressive aphasia. *Brain, 136*, 2619–2628.
Chang, S. E., Erickson, K. I., Ambrose, N. G., Hasegawa-Johnson, M. A., & Ludlow, C. L. (2008). Brain anatomy differences in childhood stuttering. *NeuroImage, 39*, 1333–1344.

Chang, S. E., Horwitz, B., Ostuni, J., Reynolds, R., & Ludlow, C. L. (2011). Evidence of left inferior frontal premotor structural and functional connectivity deficits in adults who stutter. *Cerebral Cortex, 21*, 2507–2518.
Chang, S. E., Kenney, M. K., Loucks, T. M. J., & Ludlow, C. L. (2009). Brain activation abnormalities during speech and non-speech in stuttering speakers. *NeuroImage, 46*, 201–212.
Chang, S. E., & Zhu, D. C. (2013). Neural network connectivity differences in children who stutter. *Brain, 136*, 3709–3726.
Chang, S. E., Zhu, D. C., Choo, A. L., & Angstadt, M. (2015). White matter neuroanatomical differences in young children who stutter. *Brain, 138*, 694–711.
Choo, A. L., Chang, S. E., Zengin-Bolatkale, H., Ambrose, N. G., & Loucks, T. M. (2012). Corpus callosum morphology in children who stutter. *Journal of Communication Disorders, 45*, 279–289.
Choo, A. L., Kraft, S. J., Olivero, W., Ambrose, N. G., Sharma, H., Chang, S. E., et al. (2011). Corpus callosum differences associated with persistent stuttering in adults. *Journal of Communication Disorders, 44*, 470–477.
Cieslak, M., Ingham, R. J., Ingham, J. C., & Grafton, S. T. (2015). Anomalous white matter morphology in adults who stutter. *Journal of Speech, Language, and Hearing Research, 58*, 268–277.
Civier, O., Kronfeld-Duenias, V., Amir, O., Ezrati-Vinacour, R., & Ben-Shachar, M. (2015). Reduced fractional anisotropy in the anterior corpus callosum is associated with reduced speech fluency in persistent developmental stuttering. *Brain and Language, 143*, 20–31.
Connally, E. L., Ward, D., Howell, P., & Watkins, K. E. (2014). Disrupted white matter in language and motor tracts in developmental stuttering. *Brain and Language, 6*, 256–266.
Cykowski, M. D., Fox, P. T., Ingham, R. J., Ingham, J. C., & Robin, D. A. (2010). A study of the reproducibility and etiology of diffusion anisotropy differences in developmental stuttering: A potential role for impaired myelination. *NeuroImage, 52*, 1495–1504.
Danielian, L. E., Iwata, N. K., Thomasson, D. M., & Floeter, M. K. (2010). Reliability of fiber tracking measurements in diffusion tensor imaging for longitudinal study. *NeuroImage, 49*, 1572–1580.
De Santis, S., Drakesmith, M., Bells, S., Assaf, Y., & Jones, D. K. (2014). Why diffusion tensor MRI does well only some of the time: Variance and covariance of white matter tissue microstructure attributes in the living human brain. *NeuroImage, 89*, 35–44.
Dick, A. S., Bernal, B., & Tremblay, P. (2013). The language connectome: New pathways, new concepts. *The Neuroscientist, 20*, 467–543.
Dougherty, R. F., Ben-Shachar, M., Bammer, R., Brewer, A. A., & Wandell, B. A. (2005). Functional organization of human occipital-callosal fiber tracts. *Proceedings of the National Academy of Sciences of the United States of America, 102*, 7350–7355.
Dougherty, R. F., Ben-Shachar, M., Deutsch, G. K., Hernandez, A., Fox, G. R., & Wandell, B. A. (2007). Temporal-callosal pathway diffusivity predicts phnological skills in children. *PNAS, 104*, 8556–8561.
Draganski, B., Kherif, F., Klöppel, S., Cook, P. A., Alexander, D. C., Parker, G. J., et al. (2008). Evidence for segregated and integrative connectivity patterns in the human basal ganglia. *The Journal of Neuroscience, 28*, 7143–7152.
Duffau, H., Moritz-Gasser, S., & Mandonnet, E. (2014). A re-examination of neural basis of language processing: Proposal of a dynamic hodotopical model from data provided by brain stimulation mapping during picture naming. *Brain and Language, 131*, 1–10.
Etchell, A. C., Civier, O., Ballard, K., & Sowman Paul, F. (2017). A systematic review of neuroimaging research in stuttering between 1995 and 2016. *Journal of Fluency Disorders* this issue.
Friston, K. J., & Ashburner, J. (2004). Generative and recognition models for neuroanatomy. *NeuroImage, 23*, 21–24.
Golfinopoulos, E., Tourville, J. A., & Guenther, F. H. (2010). The integration of large-scale neural network modeling and functional brain imaging in speech motor control. *NeuroImage, 52*, 862–874.
Herbet, G., Lafargue, G., Bonnetblanc, F., Moritz-Gasser, S., De Champfleur, N. M., & Duffau, H. (2014). Inferring a dual-stream model of mentalizing from associative white matter fibres disconnection. *Brain, 137*, 944–959.
Hickok, G., & Poeppel, D. (2004). Dorsal and ventral streams: A framework for understanding aspects of the functional anatomy of language. *Cognition, 92*, 67–99.
Hickok, G., & Poeppel, D. (2007). The cortical organization of speech processing. *Nature Reviews Neuroscience, 8*, 393–402.
Horowitz, A., Barazany, D., Tavor, I., Bernstein, M., Yovel, G., & Assaf, Y. (2014). In vivo correlation between axon diameter and conduction velocity in the human brain. *Brain Structure and Function,* 1–12.
Jones, D. K. (2008). Studying connections in the living human brain with diffusion MRI. *Cortex, 44*, 936–952.
Jones, D. K., Knösche, T. R., & Turner, R. (2013). White matter integrity, fiber count, and other fallacies: The do's and don'ts of diffusion MRI. *NeuroImage, 73*, 239–254.
Keedwell, P. A., Doidge, A. N., Meyer, M., Lawrence, N., Lawrence, A. D., & Jones, D. K. (2016). Subgenual cingulum microstructure supports control of emotional conflict. *Cerebral Cortex,* hw030.
Kell, C. A., Neumann, K., Kriegstein, K. V., Posenenske, C., Gudenberg, A. W. V., Euler, H., et al. (2009). How the brain repairs stuttering. *Brain, 132*, 2747–2760.
Kemerdere, R., de Champfleur, N. M., Deverdun, J., Cochereau, J., Moritz-Gasser, S., Herbet, G., et al. (2016). Role of the left frontal aslant tract in stuttering: A brain stimulation and tractographic study. *Journal of Neurology, 263*, 157–167.
Kronfeld-Duenias, V., Amir, O., Ezrati-Vinacour, R., Civier, O., & Ben-Shachar, M. (2016a). Dorsal and ventral language pathways in persistent developmental stuttering. *Cortex, 81*, 79–92.
Kronfeld-Duenias, V., Amir, O., Ezrati-Vinacour, R., Civier, O., & Ben-Shachar, M. (2016b). The frontal aslant tract underlies speech fluency in persistent developmental stuttering. *Brain Structure and Function, 221*, 365–381.
Le Bihan, D., Breton, E., Lallemand, D., Grenier, P., Cabanis, E., & Laval-Jeantet, M. (1986). MR imaging of intravoxel incoherent motions: Application to diffusion and perfusion in neurologic disorders. *Radiology, 161*, 401–407.
Lehéricy, S., Ducros, M., De Moortele, V., Francois, C., Thivard, L., Poupon, C., et al. (2004). Diffusion tensor fiber tracking shows distinct corticostriatal circuits in humans. *Annals of Neurology, 55*, 522–529.
Lehéricy, S., Ducros, M., Krainik, A., Francois, C., Van de Moortele, P. F., Ugurbil, K., et al. (2004). 3-D diffusion tensor axonal tracking shows distinct SMA and pre-SMA projections to the human striatum. *Cerebral Cortex, 14*, 1302–1309.
Lu, C., Chen, C., Ning, N., Ding, G., Guo, T., Peng, D., et al. (2010). The neural substrates for atypical planning and execution of word production in stuttering. *Experimental Neurology, 221*, 146–156.
Mandonnet, E., Nouet, A. L., Gatignol, P., Capelle, L., & Duffau, H. (2007). Does the left inferior longitudinal fasciculus play a role in language? A brain stimulation study. *Brain, 130*, 623–629.
Mauchly, J. W. (1940). Significance test for sphericity of a normal n-variate distribution. *The Annals of Mathematical Statistics, 11*, 204–209.
Mezer, A., Yeatman, J. D., Stikov, N., Kay, K. N., Cho, N.-J., Dougherty, R. F., et al. (2013). Quantifying the local tissue volume and composition in individual brains with MRI. *Nature Medicine, 19*, 1667–1672.
Mori, S., & Aggarwal, M. (2014). In vivo magnetic resonance imaging of the human limbic white matter. *Frontiers in Aging Neuroscience, 6*, 1–6.
Mori, S., Crain, B. J., Chacko, V., & Van Zijl, P. (1999). Three-dimensional tracking of axonal projections in the brain by magnetic resonance imaging. *Annals of Neurology, 45*, 265–269.
Neef, N. E., Anwander, A., & Friederici, A. D. (2015). The neurobiological grounding of persistent stuttering: From structure to function. *Current neurology and neuroscience reports, 15*, 63.
Nichols, T. E., & Holmes, A. P. (2001). Nonparametric permutation tests for functional neuroimaging: A primer with examples. *Human Brain Mapping, 15*, 1–25.
Oldfield, R. C. (1971). The assessment and analysis of handedness: The Edingburgh inventory. *Neuropsychologia, 9*, 97–113.
Ortibus, E., Verhoeven, J., Sunaert, S., Casteels, I., De Cock, P., & Lagae, L. (2012). Integrity of the inferior longitudinal fasciculus and impaired object recognition in children: A diffusion tensor imaging study. *Developmental Medicine and Child Neurology, 54*, 38–43.
Penny, W. D., Friston, K. J., Ashburner, J. T., Kiebel, S. J., & Nichols, T. E. (Eds.). (2011). *Statistical parametric mapping: The analysis of functional brain images*. Academic Press.
Pestilli, F., Yeatman, J. D., Rokem, A., Kay, K. N., & Wandell, B. A. (2014). Evaluation and statistical inference form human connectomes. *Nature Methods, 11*, 1058–1063.

Pierpaoli, C., & Basser, P. J. (1996). Toward a quantitative assessment of diffusion anisotropy. *Magnetic Resonance in Medicine, 36*, 893–906.
Riley, G. (1994). *Stuttering severity instrument for children and adults* (Third edition). Austin, Texas: Pro-Ed.
Rokem, A., Yeatman, J. D., Pestilli, F., Kay, K. N., Mezer, A., van der Walt, S., et al. (2015). Evaluating the accuracy of diffusion MRI models in white matter. *PloS one, 10*, e0123272.
Schmahmann, J. D., Pandya, D. N., Wang, R., Dai, G., D'Arceuil, H. E., de Crespigny, A. J., et al. (2007). Association fibre pathways of the brain: Parallel observations from diffusion spectrum imaging and autoradiography. *Brain, 130*, 630–653.
Sherbondy, A., Dougherty, R. F., Ben-Shachar, M., Napel, S., & Wandell, B. A. (2008). ConTrack: Finding the most likely pathways between brain regions using diffusion tractography. *Journal of Vision, 15*, 1–16.
Sitek, K. R., Cai, S., Beal, D. S., Perkell, J. S., Guenther, F. H., & Ghosh, S. S. (2016). Decreased cerebellar-orbitofrontal connectivity correlates with stuttering severity: Whole-brain functional and and structural connectivity associations with persistent developmental stuttering. *Frontiers in Human Neuroscience, 10*, 190.
Smith, S. M., Jenkinson, M., Johansen-Berg, H., Rueckert, D., Nichols, T. E., Mackay, C. E., et al. (2006). Tract-based spatial statistics: Voxelwise analysis of multi-subject diffusion data. *NeuroImage, 31*, 1487–1505.
Sommer, M., Koch, M. A., Paulus, W., Weiller, C., & Büchel, C. (2002). Disconnection of speech-relevant brain areas in persistent developmental stuttering. *The Lancet, 360*, 380–383.
Stikov, N., Perry, L. M., Mezer, A., Rykhlevskaia, E., Wandell, B. A., Pauly, J. M., et al. (2011). Bound pool fractions complement diffusion measures to describe white matter micro and macrostructure. *NeuroImage, 54*, 1112–1121.
Tavor, I., Yablonski, M., Mezer, A., Rom, S., Assaf, Y., & Yovel, G. (2014). Separate parts of occipito-temporal white matter fibers are associated with recognition of faces and places. *NeuroImage, 86*, 123–130.
Thiebaut de Schotten, M., Dell'Acqua, F., Valabregue, R., & Catani, M. (2012). Monkey to human comparative anatomy of the frontal lobe association tracts. *Cortex, 48*, 82–96.
Tournier, J.-D., Yeh, C.-H., Calamante, F., Cho, K.-H., Connelly, A., & Lin, C.-P. (2008). Resolving crossing fibres using constrained spherical deconvolution: Validation using diffusion-weighted imaging phantom data. *NeuroImage, 42*, 617–625.
Tournier, J. D., Calamante, F., Gadian, D. G., & Connelly, A. (2004). Direct estimation of the fiber orientation density function from diffusion-weighted MRI data using spherical deconvolution. *NeuroImage, 23*, 1176–1185.
Tournier, J. D., Mori, S., & Leemans, A. (2011). Diffusion tensor imaging and beyond. *Magnetic Resonance in Medicine, 65*, 1532–1556.
Travis, K. E., Adams, J. N., Ben-Shachar, M., & Feldman, H. M. (2015). Decreased and increased anisotropy along major cerebral white matter tracts in preterm children and adolescents. *PLoS One, 10*, e0142860.
Tuch, D. S. (2004). Q-ball imaging. *Magnetic Resonance in Medicine, 52*, 1358–1372.
Wakana, S., Caprihan, C., Panzenboeck, M. M., Fallon, J. H., Perry, M., Gollub, R. L., et al. (2007). Reproducibility of quantitative tractography methods: Applied to cerebral white matter. *NeuroImage, 36*, 630–644.
Watkins, K. E., Smith, S. M., Davis, S., & Howell, P. (2008). Structural and functional abnormalities of the motor system in developmental stuttering. *Brain, 131*, 50–59.
Wedeen, V. J., Hagmann, P., Tseng, W.-Y. I., Reese, T. G., & Weisskoff, R. M. (2005). Mapping complex tissue architecture with diffusion spectrum magnetic resonance imaging. *Magnetic Resonance in Medicine, 54*, 1377–1386.
Xuan, Y., Meng, C., Yang, Y., Zhu, C., Wang, L., Yan, Q., et al. (2012). Resting-state Brain activity in adult males who stutter. *PloS one, 7*, e30570.
Yairi, E., & Ambrose, N. (1999). Early childhood stuttering I: Persistency and recovery rates. *Journal of speech, Language and Hearing research, 35*, 755–760.
Yeatman, J. D., Dougherty, R. F., Myall, N. J., Wandell, B. A., & Feldman, H. M. (2012). Tract profiles of white matter properties: Automating fiber-tract quantification. *PLoS One, 7*, e49790.
Yeatman, J. D., Dougherty, R. F., Rykhlevskaia, E., Sherbondy, A. J., Deutsch, G. K., Wandell, B. A., et al. (2011). Anatomical properties of the arcuate fasciculus predict phonological and reading skills in children. *Journal of Cognitive Neuroscience, 23*, 3304–3317.

Dr. Kronfeld-Duenias investigates the brain structure-to-function relations, with a particular interest in speech and language processing. She has completed her undergraduate studies in Tel-Aviv University, where she joined The Functional Brain Imaging Unit at the Sourasky Medical Center to study white matter structures in young children with autism. She then conducted her PhD. at The Bar-Ilan University, where she studied the neural correlates of persistent developmental stuttering. Currently, Dr. Kronfeld-Duenias is a postdoctoral fellow at Prof. Yaniv Assaf's lab in Tel-Aviv University.

Dr. Civier received his PhD from Boston University. Under the supervision of Prof. Frank Guenther, he used computational modeling to investigate the neural substrates of stuttering and induced fluency. In his postdoctoral fellowship in Dr. Michal Ben-Shachar's Neurolinguistics lab at Bar-Ilan University, he studied white matter and functional anomalies in stuttering. Dr. Civier also investigated manual and speech motor control using MEG and motion-tracking cameras at the Weizmann Institute of Science. Currently, Dr. Civier is a postdoctoral fellow in the Florey Institute of Neuroscience and Mental Health, where he develops tools to study the brain's structural and functional connectivity.

Prof. Amir is the head of the Department of Communication Disorders at Tel-Aviv University. He has completed his undergraduate and graduate studies in Tel-Aviv University and earned his doctoral degree in the Dept. of Speech and Hearing sciences, at the University of Illinois (USA) in 1998. In addition to his academic activities, Prof. Amir heads a private practice, where he diagnoses and treats people who stutter and people with voice disorders. Furthermore, Prof. Amir volunteers, as a senior voice and speech therapist, at the Speech and Hearing Center, and at the Voice Clinic, at the 'Sheba' Medical Center.

Dr. Ezrati-Vinacour is a senior lecturer at the Department of Communication Disorders at Tel Aviv University. She has conducted her MA and PhD at Tel Aviv University, where she studied the link between stuttering manifestations, anxiety levels and the ability to estimate time. Then, she pursued a postdoc fellowship at the University of Illinois, Urbana-Champaign under the direct supervision Prof. Ehud Yairi. A part from her academic career, Dr. Ezrati-Vinacour runs a private clinic, where she diagnoses and treats people who suffer from speech disfluencies.

Dr. Ben-Shachar is a faculty member at the Department of English Literature and Linguistics, and the head of the Neurolinguistics Lab at the Gonda Multidisciplinary Brain Research Center in Bar-Ilan University. Dr. Ben-Shachar completed her MA and PhD studies in Tel-Aviv University, where she studied brain systems involved in syntactic processing using fMRI. She then pursued a postdoctoral position at Stanford University, examining reading and brain development in children. Her lab in Bar Ilan University studies the neural systems that underlie language and reading, in typical and atypical populations, using diffusion MRI, fMRI and behavioral methods.